# Lysine 5 and Phenylalanine 9 of the Factor IX $\omega$-Loop Interact with Phosphatidylserine in a Membrane-Mimetic Environment†

Marianne A. Grant,‡ Roustem F. Baikeev,§ Gary E. Gilbert,*,§ and Alan C. Rigby*,‡

*Division of Hemostasis and Thrombosis, Beth Israel Deaconess Medical Center, and Department of Medicine, Harvard Medical School, 330 Brookline Avenue, Boston, Massachusetts 02215, and Medicine Department of VA Hospital, Brigham and Women's Hospital, and Harvard Medical School, 1400 VFW Parkway, West Roxbury, Massachusetts 02132*

*Received May 3, 2004; Revised Manuscript Received September 16, 2004*

ABSTRACT: The binding of factor IX to cell membranes requires a structured N-terminal $\omega$-loop conformation that exposes hydrophobic residues for a highly regulated interaction with a phospholipid. We hypothesized that a peptide comprised of amino acids Gly4−Gln11 of factor IX ($fIX_{G4-Q11}$) and constrained by an engineered disulfide bond would assume the native factor IX $\omega$-loop conformation in the absence of $Ca^{2+}$. The small size and freedom from aggregation-inducing calcium interactions would make $fIX_{G4-Q11}$ suitable for structural studies for eliciting details about phospholipid interactions. $fIX_{G4-Q11}$ competes with factor IXa for binding sites on phosphatidylserine-containing membranes with a $K_i$ of 11 $\mu$M and inhibits the activation of factor X by the factor VIIIa−IXa complex with a $K_i$ of 285 $\mu$M. The NMR structure of $fIX_{G4-Q11}$ reveals an $\omega$-loop backbone fold and side chain orientation similar to those found in the calcium-bound factor IX Gla domain, FIX(1−47)−$Ca^{2+}$. Dicaproylphosphatidylserine ($C_6$-PS) induces HN, H$\alpha$ backbone, and H$\beta$ chemical shift perturbations at residues Lys5, Leu6, Phe9, and Val10 of $fIX_{G4-Q11}$, while selectively protecting the NH$\zeta$ side chain resonance of Lys5 from solvent exchange. NOEs between the aromatic ring protons of Phe9 and specific acyl chain protons of $C_6$PS indicate that these phosphatidylserine protons reside 3−6 Å from Phe9. Stabilization of the phosphoserine headgroup and glycerol backbone of $C_6$PS identifies that phosphatidylserine is in a protected environment that is spatially juxtaposed with $fIX_{G4-Q11}$. Together, these data demonstrate that Lys5, Leu6, Phe9, and Val10 preferentially interact with $C_6$PS and allow us to correlate known hemophilia B mutations of factor IX at Lys5 or Phe9 with impaired phosphatidylserine interaction.

Factor IX is the zymogen precursor for factor IXa, an essential enzyme of blood coagulation. Factor IXa functions in a membrane-bound enzyme complex with factor VIIIa, the tenase (Xase) complex, which activates factor X to factor Xa. The importance of factor IXa in hemostasis is demonstrated by the severe bleeding abnormality, hemophilia B, which is associated with factor IX deficiency or altered factor IXa activity. Phosphatidylserine-containing membranes are essential to blood coagulation in providing a molecular surface for the assembly of enzyme−cofactor complexes which efficiently convert circulating zymogens to active enzymes, and also act as an activator of the assembled complexes (*1*).

Factor IX is a member of the vitamin K-dependent family of serine proteases that is comprised of enzymes and cofactors that are critical for regulating the blood coagulation cascade, including but not limited to prothrombin, factor X, protein C, and protein S (reviewed in refs *2*−*5*). It is well-established that the vitamin K-dependent proteins in plasma bind to phosphatidylserine-containing membranes through a mechanism involving the N-terminal $\gamma$-carboxyglutamic acid (Gla)[1] domain (*6*, *7*). This domain is comprised of approximately 45 residues and is rich in Gla, a posttranslationally modified glutamic acid residue possessing a malonate-like side chain that chelates divalent metal ions (*8* and references therein). These Gla domains are comprised of 9−13 Gla residues which bind calcium ions, inducing a significant structural perturbation from a largely unfolded domain to the folded membrane-binding conformer (*9*−*12*). This calcium-dependent, membrane-binding conformer ex-

† This study was supported by separate grants from the American Heart Association National Center and NIH Grant RO1 HL67212 to A.C.R., from the National Institutes of Health to M.A.G. (HL10484). G.E.G. and R.F.B. were supported by the Department of Veterans Affairs and NIH Grant P01 HL42443.

* To whom correspondence should be addressed. A.C.R.: Division of Hemostasis and Thrombosis, 330 Brookline Ave., Boston, MA 02215; telephone, (617) 667-0637; fax, (617) 975-5505, e-mail, arigby@bidmc.harvard.edu. G.E.G.: Medicine Department of VA Hospital, OREA Bldg., Rm. 2A110, 1400 VFW Parkway, West Roxbury, MA 02132; telephone, (617) 363-5686; fax, (617) 363-5592; e-mail, ggilbert@rics.bwh.harvard.edu.

‡ Beth Israel Deaconess Medical Center and Harvard Medical School.

§ Brigham and Women's Hospital and Harvard Medical School.

[1] Abbreviations: Gla, $\gamma$-carboxyglutamic acid; NMR, nuclear magnetic resonance; HPLC, high-performance liquid chromatography; FITC, fluorescein-EGR-chloromethyl ketone; DPC, dodecylphosphatidylcholine; $C_6$PS, dicaproylphosphatidylserine; TOCSY, total correlation spectroscopy; NOESY, nuclear Overhauser enhancement spectroscopy; TFA, trifluoroacetic acid; PC, phosphatidylcholine; PS, phosphatidylserine; PE, phosphatidylethanolamine; rmsd, root-mean-square deviation; EDTA, ethylenediaminetetraacetic acid; lysoPS, lysophosphatidylserine; CMC, critical micelle concentration.

10.1021/bi049107f CCC: $27.50 
Published on Web 11/12/2004

presses a solvent-exposed loop of hydrophobic amino acids within the ~12 N-terminal residues (*13*, *14*). This portion of the Gla domain has been identified as an $\omega$-loop on the basis of its conformation, hydrophobic character, and solvent exposure (*15*).

Several investigations thus far have demonstrated that the solvent-exposed hydrophobic residues of the Gla domain $\omega$-loop have important roles in phospholipid membrane binding (*14*, *16*−*19*). However, these requisite phosphatidylserine-specific interactions underlying membrane binding have not been completely identified (*6*). Recent X-ray crystallographic structures of bovine prothrombin fragment 1 and heteronuclear NMR spectroscopy studies of a selectively $^{15}$N-labeled peptide comprised of the human prothrombin Gla domain, PT(1−46), in complex with calcium, and calcium with lysophosphatidylserine (lysoPS), have facilitated the identification of critical recognition epitopes for both the prothrombin Gla domain and lysoPS (*12*). The conformational selection and structural rigidity that are induced in the $\omega$-loop following phospholipid binding are the result of several interactions between the glycerol backbone and acyl chain of the bound lysoPS and the prothrombin Gla domain $\omega$-loop (*12*). Specifically, the side chain of Lys3 is conformationally fixed in the presence of lysoPS through interactions between the NH$\zeta$ group of this residue and all three acyl oxygen atoms of the lipid. In addition, the side chain of Phe5 is locked into a single conformation in the PT(1−46)−$Ca^{2+}$−lysoPS ternary complex. These data illustrate with atomic resolution the importance of the $\omega$-loop N-terminal residues in prothrombin for binding to lysoPS.

A synthetic cyclic peptide incorporating amino acids Gly4−Gln11 of human factor IX ($fIX_{G4-Q11}$) was used to probe the contribution of the factor IX $\omega$-loop in factor IX/factor IXa−platelet membrane interactions (*20*). These studies demonstrated that this cyclic $\omega$-loop peptide was responsible for mediating binding of factor IX/factor IXa to platelet membranes. In this study, we have utilized this peptide to evaluate the membrane binding properties of the factor IX $\omega$-loop. Specifically, we have used one-dimensional (1D) and two-dimensional (2D) NMR spectroscopy to determine the structure of this conformationally constrained $\omega$-loop peptide. We then utilized these structural data as a platform to investigate interactions with phosphatidylserine. Our data demonstrate that $fIX_{G4-Q11}$ is constrained into an $\omega$-loop-like, membrane-binding conformation in which residues Lys5, Leu6, Phe9, and Val10 preferentially interact with phosphatidylserine. In addition, these data show specific interactions between phosphatidylserine and the side chains of Lys5 and Phe9 in $fIX_{G4-Q11}$, results that help us to better understand naturally occurring factor IX mutations of Lys5 and Phe9 in patients with hemophilia B.

## EXPERIMENTAL PROCEDURES

*Materials.* Dodecylphosphocholine-$d_{38}$ (DPC) was from Cambridge Isotope Laboratories (Andover, MA) and dodecylphosphocholine from Anatrace (Maumee, OH). Dicaproylphosphatidylserine ($C_6$PS), bovine brain phosphatidylserine, egg yolk phosphatidylcholine, and egg yolk phosphatidylethanolamine were from Avanti Polar Lipids (Alabaster, AL). Human factor X, human factor IXa, and human factor IIa were from Enzyme Research Laboratories (South Bend, IN). Recombinant human factor VIII was a gift from D. Pittman of Genetics Institute (Cambridge, MA). Chromogenic substrate S-2765 was from DiaPharma Group (West Chester, OH).

*Chemical Synthesis of the $fIX_{G4-Q11}$ Peptide.* The $fIX_{G4-Q11}$ peptide was synthesized using FMOC/*N*-methylpyrrolidone chemistry on an Applied Biosystems model 430A peptide synthesizer. Amino acids were coupled as 1-hydroxybenzotriazole esters onto *p*-hydroxymethylphenoxymethyl polystyrene resin preloaded with cysteine (Applied Biosystems, Foster City, CA). Each amino acid coupling proceeded for a total of 91 min with constant vortexing. Following each coupling, all uncoupled $\alpha$-$NH_2$ termini were acetylated. After removal of the amino acid solution and after being washed with *N*-methylpyrrolidone (NMP), the residues were deprotected with a 20% piperidine/NMP mixture in a 30 min reaction. Five NMP washes preceded the next amino acid addition. Cleavage of the peptide from its solid support and simultaneous side chain deprotection were performed using a trifluoroacetic acid/water/thioanisole/phenol/1,2-ethanedithiol cocktail (82.5:5:5:5:2.5). The cleavage reaction was allowed to proceed for 5 h at 25 °C with constant stirring. Following removal of the resin via filtration, 50 mL of dichloromethane was added to the cleavage reaction mixture prior to concentration by rotary evaporation. The crude peptide was precipitated using cold anhydrous ethyl ether and washed several times with ethyl ether prior to drying *in vacuo*.

$fIX_{G4-Q11}$ was cyclized via oxidative disulfide bond formation between the N- and C-terminal cysteines by exhaustive dialysis against 50 mM ammonium bicarbonate at pH 8.0 and 4 °C for 4 days. The crude peptide was purified by HPLC using a reverse-phase C18 column (Vydac, 250 mm × 21.5 mm) with a linear gradient of acetonitrile in 0.1% trifluoroacetic acid. The amino acid sequence was verified using an Applied Biosystems model 491A protein sequencer. Molecular masses were determined by MALDI-TOF mass spectrometry on a Voyager linear MALDI-TOF spectrometer (PerSeptive Biosystems, Foster City, CA) employing linear mode-positive ionizations. An Ellman's assay was performed to determine that all disulfides were oxidized within refolded $fIX_{G4-Q11}$ (*21*). Complete oxidation of $fIX_{G4-Q11}$ was further demonstrated using excess iodoacetamide. The subsequent reaction products were separated using reverse-phase $C_{18}$ HPLC and analyzed by MALDI-TOF mass spectrometry.

*Preparation of Phospholipid Vesicles.* Phospholipid vesicles with a specific composition were prepared using molar ratios of each lipid dissolved in chloroform (100% PC; 20% PS and 80% PC; 15% PS, 20% PE, and 65% PC; or 20% PS, 20% PE, and 60% PC). The chloroform was evaporated under a stream of nitrogen gas, and the lipid film was resuspended in methylene chloride and then evaporated thrice under argon gas. Phospholipids were then suspended by gently swirling Tris-buffered saline [50 mM Tris (pH 7.4) and 150 mM NaCl] over the dried lipid suspension until the entire lipid was suspended. Vesicles prepared this way were then sonicated in a high-intensity bath sonicator until they were clear (*22*). Vesicles were used fresh, or 1 mL aliquots were flash-frozen in liquid nitrogen, stored at −80 °C, and thawed at 37 °C. The duration of the storage at 4 °C before incubation with glass microspheres did not exceed 4 h.

*Fluorescein-Glu-Gly-Arg Chloromethyl Ketone Labeling of Factor IXa (FITC−IXa).* Factor IXa was labeled with fluorescein-Glu-Gly-Arg chloromethyl ketone (Haematologic Technologies), essentially as described for the dansyl-Glu-Gly-Arg chloromethyl ketone labeling of factor IX (*23*). The free fluorescein-labeled peptide was removed by centrifugal filtration using a Centricon-30 device (Millipore, Waltham, MA). Labeling efficiency was determined by comparing the ratio of the absorbance at 280 nm to the absorbance at 490 nm, divided by extinction coefficients for factor IXa and fluorescein.

*Flow Cytometry Binding Assay.* Lipospheres were prepared as previously described (*24*). Glass microspheres 1.6 μm in diameter (Duke Scientific, Palo Alto, CA) were size-restricted and incubated with sonicated vesicles of a chosen composition, and washed thrice in 20 mM Tris-HCl (pH 7.5), 150 mM NaCl, 0.1% defatted bovine albumin, and 10 μM egg PC in vesicles. Lipospheres were stored at 4 °C and used within 4 h of preparation. Fluorescein-labeled factor IXa (128 nM) was incubated with $fIX_{G4-Q11}$ for 15 min at room temperature; the mixture was added to lipospheres for an additional 10 min, and the amount of membrane-bound fluorescein-labeled factor IXa was measured by flow cytometry. This procedure was performed on 25 μL aliquots of the 125 μL sample with an approximate liposphere concentration of $1 \times 10^6$ $mL^{-1}$ using a Becton Dickinson (San Jose, CA) FACS Calibur flow cytometer. Forward light scatter triggered data acquisition with all photomultipliers in the log mode. Noise was reduced during analysis by eliminating events with forward and side scatter values different from those characteristic of the lipospheres. The mean log fluorescence was converted to linear fluorescence as reported in the figures. Only experiments in which the fluorescence histogram indicated a normal log distribution, as judged by inspection, were analyzed quantitatively. Flow cytometry experiments were performed in 20 mM Tris-HCl (pH 7.5), 140 mM NaCl, 5 mM $CaCl_2$, and 0.1% bovine albumin. We determined the inhibition constant ($K_i$) for $fIX_{G4-Q11}$ using Prizm 3.0 software (GraphPad Software, Inc., San Diego, CA) and the equation of Cheng and Prusoff (*25*), where a predetermined $K_d$ (1000 nM) for binding of factor IXa to bovine brain vesicles (33% PS/33% PE/33% PC) was used (*26*). The level of residual nonspecific binding of labeled factor IXa to 100% PC lipospheres was subtracted from the total bound. $fIX_{G4-Q11}$ competed for a single population of saturable binding sites on the lipospheres. In the estimation of the $IC_{50}$ and $K_i$ values, the $IC_{50}$ of $fIX_{G4-Q11}$ represents the concentration of $fIX_{G4-Q11}$ capable of displacing 50% of the displaceable labeled factor IXa molecules.

*Factor Xase Assay.* The activation of factor X by factor IXa in the presence of $fIX_{G4-Q11}$ and in the presence or absence of phospholipids was assessed using a two-step amidolytic substrate assay (*1*) with the following modifications. Factor IXa (0.125 nM) was incubated with factor X (0.13 μM), phospholipids (1 μM) with a 20% PS/80% PC composition, and varied concentrations of $fIX_{G4-Q11}$ in 50 mM Tris-HCl (pH 7.4), 150 mM NaCl, 1.5 mM $CaCl_2$, 1 nM factor VIII, and 0.19 nM thrombin for 5 min at 25 °C. In the absence of phospholipids, it was necessary to increase the concentration of factor IXa, factor X, and factor VIII (40 nM factor IXa, 500 nM factor X, and 40 nM factor VIII). Final reaction volumes were 40 μL. The reaction was stopped by the addition of EDTA to a final concentration of 7 mM. The amount of factor Xa generated was determined immediately using the chromogenic substrate S-2765 (0.31 mg/mL) on a Molecular Devices (Sunnyvale, CA) microplate plate reader in the kinetic mode. The results represent the mean of triplicates from a representative experiment. The derivation of $K_i$ in the case of inhibition of factor X activation by $fIX_{G4-Q11}$, based on a one-enzyme, one-substrate model, was analyzed by Dixon plots as previously described (*27*).

*Circular Dichroism.* Lyophilized $fIX_{G4-Q11}$ was dissolved in 5 mM $Na_2HPO_4$ and 5 mM $NaH_2PO_4$ (pH 7.4) to a final concentration of 67.2 μM. The CD spectra of $fIX_{G4-Q11}$ were collected on a JASCO 810 spectropolarimeter (Jasco Inc., Easton, MD) equipped with a thermoelectric temperature control unit in buffer alone, dodecylphosphocholine (DPC) micelles, mixed dicaproylphosphatidylserine ($C_6PS$)/DPC (13:87) micelles, and phospholipid vesicles (20% PS/20% PE/60% PC) in the absence and presence of 1.1 mM $CaCl_2$. The spectrometer was calibrated using a standard of D-(+)-10-camphorsulfonic acid. Spectra were recorded as single scans between 195 and 260 nm using a path length of 0.1 cm, a dwell time of 5 s/nm, and a temperature of 37 °C. All spectra were corrected for light scatter by buffer subtraction. Results are expressed in terms of molar ellipticity in units of degrees, square centimeter per mole.

*NMR Spectroscopy of $fIX_{G4-Q11}$.* NMR structures were determined from several two-dimensional (2D) $^1H$ NMR data sets recorded over a temperature range from 5 to 25 °C on a 500 MHz Varian Unity INOVA spectrometer with a proton frequency of 499.695 MHz. The final data set used to determine the three-dimensional structure of $fIX_{G4-Q11}$ was collected at 15 °C. Samples contained 3 mM synthetic $fIX_{G4-Q11}$ peptide and 200 mM dodecylphosphocholine-$d_{38}$ micelles in 90% $H_2O$ and 10% $D_2O$ (pH 5.6). The carrier frequency was set to the water resonance, which was suppressed using presaturation during the preacquisition delay.

Final 2D NOESY spectra were recorded with mixing times of 250 and 350 ms at 15 °C. A total of 4096 real data points were acquired in $t_2$, and 384 time-proportional phase increments (TPPIs) were implemented in $t_1$ with a spectral width of 8000 Hz in the $F_2$ dimension. A total of 128 summed transients were collected with a relaxation delay of 1.2 s. Additional NOESY data were acquired with samples initially lyophilized and then reconstituted in 99.996% $D_2O$ (Cambridge Isotope Laboratories) at a noncorrected pH of 5.6 to complete the assignments of resonances located near the water peak and to discern weak NOE cross-peaks.

2D TOCSY spectra were recorded with a mixing time of 35 or 45 ms at 15 °C using the MLEV-17 spin-lock sequence (*28*, *29*). A total of 4096 real data points were acquired in $t_2$, and 384 TPPIs were implemented in $t_1$ with a spectral width of 8000 Hz in the $F_2$ dimension. A total of 192 summed transients were collected with a relaxation delay of 1.2 s. Spectra were processed off-line with Gaussian and sine bell functions for apodization in $t_2$ and a shifted sine bell function in $t_1$ using VNMR (Varian, Inc., Palo Alto, CA). All data were zero-filled to 4K by 2K real matrices. A 2D DQF-COSY spectrum was acquired with 4096 real data points in $t_2$, and 640 TPPIs were implemented in $t_1$ with a spectral width of 8000 Hz in the $F_2$ dimension. A total of 96 summed transients were collected for measurement of

$^3J_{NH\alpha}$ spin−spin coupling constants to derive dihedral torsion angles. A natural abundance $^{13}C-^1H$ heteronuclear single-quantum coherence spectrum (HSQC) was acquired with 1024 real data points in $t_2$ and 160 TPPIs implemented in $t_1$ with a spectral width of 17591 Hz in the $F_2$ dimension to verify amino acid assignments and evaluate the prolyl−peptide bond conformations.

*Proton Resonance Assignments.* Spin-system identifications of $fIX_{G4-Q11}$ proton resonances in the presence of DPC were completed using DFQ-COSY and TOCSY experiments, which provided $^1H-^1H$ through-bond connectivities to identify specific spin systems. For sequence-specific assignments, sequential $d_{\alpha N}$, $d_{\beta N}$, and $d_{NN}$ NOE connectivities obtained from NOESY experiments were used and facilitated the complete assignment of this peptide. The vicinal spin−spin coupling constants, $^3J_{NH\alpha}$, which were less than 6.3 Hz or greater than 8.0 Hz, were used to calculate backbone $\phi$ torsion angles (*30*). NOE cross-peak intensities were classified as strong, medium, or weak and converted to distance restraint upper bounds of 2.5, 3.5, and 6.0 Å, respectively (*31*). Scalar reference peaks were chosen from nonoverlapped NH−αH NOE peaks and set to distances of 2.8 Å for calibration of the entire set of distance restraints (*32*). Where possible, rotamers of $\chi_1$ angles were categorized as either 60°, 180°, or −60° using a qualitative analysis of $\beta$-proton three-bond coupling ($^3J_{H\alpha\beta*}$) and NOE intensities, $d_{\alpha\beta1}$, $d_{\alpha\beta2}$, $d_{N\beta1}$, and $d_{N\beta2}$ (*31*). Stereospecific assignments were determined for the side chain of Leu6. Non-stereospecifically assigned atoms were treated as pseudoatoms and given correction distances (*32*). A $^{13}C-^1H$ heteronuclear single-quantum coherence spectrum (HSQC) was recorded to verify the amino acid assignments and to determine the prolyl−peptide bond conformations via the chemical shift difference between the $C_\beta$ and $C_\gamma$ resonances (*33*, *34*).

*Structure Calculations.* The structure of $fIX_{G4-Q11}$ in the presence of 200 mM DPC-$d_{38}$ was determined from 2D $^1H$ NMR spectra recorded at 15 °C. A total of 192 distance restraints and six torsion angle restraints and 11 chiral restraints were entered into the distance geometry program, DGII (CVFF force field parameters), of InsightII (Accelrys, San Diego, CA) to generate 75 final structures using a combination of simulated annealing and distance geometry (*35*). A convergent family of structures was represented by 25 conformations that demonstrated no distance violations greater than 0.3 Å, and this ensemble was used to determine the average structure for $fIX_{G4-Q11}$ using the Analysis program of InsightII. Average root-mean-squared deviations (rmsds) following superimposition of the backbone heavy atoms of each structure with the geometric average reflected the quality of the determined structures.

*Titration of $C_6$PS into $fIX_{G4-Q11}$ in DPC Micelles.* To prepare $fIX_{G4-Q11}$ samples for titration with phosphatidylserine, deuterated $C_6$PS-$d_{22}$ (Avanti Polar Lipids) that was dissolved in chloroform was dried down under nitrogen gas, resuspended in methylene chloride, and redried a total of three times. A 500 $\mu$L aliquot of 3 mM $fIX_{G4-Q11}$ peptide resuspended in 200 mM DPC-$d_{38}$ in a 90% $H_2O$/10% $D_2O$ mixture at pH 5.6 was added to the dried $C_6$PS-$d_{22}$ lipid, and the sample was warmed to 37 °C and briefly bath sonicated on ice. Before data were collected, the pH was adjusted to 5.6 with NaOH. To monitor chemical shift perturbation as a function of $C_6$PS lipid, 2D TOCSY spectra were collected at 15 °C for each titration point. For 2D NOESY experiments, protonated $C_6$PS (sodium salt) (Avanti Polar Lipids) (final concentration of 30 mM) was added to 200 mM DPC-$d_{38}$ with 3 mM $fIX_{G4-Q11}$ in either a 90% $H_2O$/10% $D_2O$ or 100% $D_2O$ solution at pH 5.6 and prepared as described above. A comparison of NOESY spectra collected with $fIX_{G4-Q11}$ in the presence of DPC alone to spectra collected in DPC with protonated $C_6$PS allowed us to identify intermolecular cross-peaks between the PS lipid moiety and the peptide.

Table 1: Synthetic Cyclic Peptides Derived from the Factor IX Gla Domain

| | | | 4 | 5 | 6 | 7 | 8 | 9 | 10 | 11 | | |
|---|---|---|---|---|---|---|---|---|---|---|---|---|
| human FIX | | | **G** | **K** | **L** | **$\gamma^a$** | **$\gamma^a$** | **F** | **V** | **Q** | | |
| $fIX_{G4-Q11}$ | C | P | **G** | **K** | **L** | D | E | **F** | **V** | **Q** | P | C |
| $fIX_{SCR}$ | C | P | E | F | G | L | Q | K | **V** | D | P | C |

[a] $\gamma$ is $\gamma$-carboxyglutamic acid (Gla).

## RESULTS

The affinity of $fIX_{G4-Q11}$ for activated platelets implies that the engineered disulfide bond constrains this $\omega$-loop-like peptide to assume the native conformation (*20*). Initial studies were focused on evaluating our working hypothesis, that the native factor IX $\omega$-loop conformation and phospholipid binding properties result from the disulfide bond constraint in $fIX_{G4-Q11}$.

*Synthesis and Characterization of $fIX_{G4-Q11}$.* $fIX_{G4-Q11}$ is based on residues Gly4−Gln11 of human factor IX (Table 1); Gla7 and Gla8 are replaced with Asp and Glu, respectively. The peptide contains complementary N-terminal and C-terminal cysteine−proline residues that provide the disulfide bond constraint (*20*). The $fIX_{G4-Q11}$ peptide was synthesized using FastMOC/*N*-methylpyrrolidone chemistry as previously described for the Gla domain of factor IX, FIX-(1−47) (*36*). Deprotected $fIX_{G4-Q11}$ was purified by reverse-phase HPLC, and the amino acid sequence was confirmed by automated Edman degradation and amino acid analysis (data not shown). Complete air oxidation of the disulfide bond in $fIX_{G4-Q11}$ was confirmed using an Ellman's assay that determined less than 2% of the sulfhydral groups were free (*21*). The molecular mass of oxidized $fIX_{G4-Q11}$, determined by MALDI-TOF mass spectrometry, is 1333.5 Da, which is in agreement with the theoretical molecular mass of $fIX_{G4-Q11}$.

*Membrane Binding of $fIX_{G4-Q11}$.* $fIX_{G4-Q11}$ was examined for its ability to compete with human factor IXa for phospholipid binding sites in a system of purified components (Figure 1A). Various concentrations of $fIX_{G4-Q11}$ were mixed with fluorescein-labeled factor IXa prior to the addition of phospholipid bilayers supported by glass microspheres (liposphereres). The membranes were comprised of 15% PS, 20% PE, and 65% PC. The results demonstrate that $fIX_{G4-Q11}$ inhibits binding of factor IXa to liposphereres with an $IC_{50}$ value of 13 ± 6 $\mu$M, and a calculated $K_i$ value of 11 ± 6 $\mu$M. These data indicated that $fIX_{G4-Q11}$ is capable of competing for 60% of the phospholipid sites recognized by factor IXa. This degree of competition is consistent with the competition previously reported for factor IX binding sites on activated platelets in which $fIX_{G4-Q11}$ and various analogues were capable of displacing 50−70% of $^{125}I$-labeled human factor IXa (*20*).

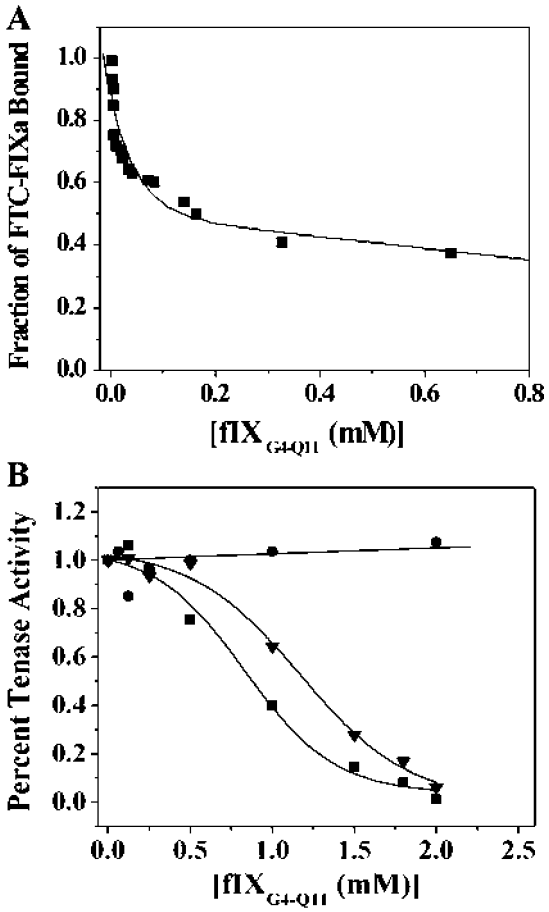


FIGURE 1: Characterization of $fIX_{G4-Q11}$ phospholipid binding. (A) The ability of $fIX_{G4-Q11}$ to inhibit binding of FITC−FIXa to lipospheres comprised of 15% PS, 20% PE, and 65% PC was determined by flow cytometry as follows. Increasing concentrations of $fIX_{G4-Q11}$ were preincubated for 15 min with 128 nM FITC−FIXa in Tris-buffered saline (pH 7.5) with 5 mM $CaCl_2$, and then this mixture was added to lipospheres and incubated for 10 min. Liposphere-bound FITC−FIXa was assessed by flow cytometry. (B) The ability of $fIX_{G4-Q11}$ to inhibit generation of factor Xa by the tenase complex was determined as follows. Increasing concentrations of $fIX_{G4-Q11}$ in 50 mM Tris-HCl (pH 7.4), 150 mM NaCl, 1.5 mM $CaCl_2$, 1 nM FVIII, and 0.19 nM thrombin were incubated at 25 °C in the presence (■) of 1 $\mu$M 20% PS/80% PC vesicles with FIXa (0.125 nM) and FX (0.13 $\mu$M) or in the absence (●) of vesicles with FIXa (40 nM) and FX (0.5 $\mu$M), where the FVIII concentration (40 nM) was also increased. Reactions were stopped by the addition of excess EDTA. FXa generation was quantitated using chromogenic substrate S-2765 which was observed by the absorbance change at 405 nm. The ability of $fIX_{SCR}$ (▼) to inhibit generation of factor Xa by the tenase complex in the presence of 1 $\mu$M 20% PS/80% PC vesicles was determined in the same manner that was used for $fIX_{G4-Q11}$.

To determine whether $fIX_{G4-Q11}$ inhibits the Xase complex by competing for functionally important binding sites in a purified system, we measured the rate of factor Xa formation with varying concentrations of $fIX_{G4-Q11}$ (Figure 1B). $fIX_{G4-Q11}$ inhibited the activation of factor X by factor IXa in the presence of factor VIII and phospholipid vesicles (20% PS/80% PC). A Dixon plot of these data confirmed that $fIX_{G4-Q11}$ is a competitive inhibitor with a $K_i$ of 285 ± 62 $\mu$M (data not shown). These data are consistent with data presented elsewhere ($K_i = 165 \pm 35$ $\mu$M) in which $fIX_{G4-Q11}$ was a competitive inhibitor of factor Xa formation in the presence of the factor Xase complex on a platelet surface (*20*). Furthermore, no inhibition was observed in the absence of phospholipid vesicles (Figure 1B), consistent with the hypothesis that inhibition of the Xase complex by $fIX_{G4-Q11}$ is due to competition for phospholipid membrane binding sites recapitulated in our purified system.

The experiments described above were repeated with $fIX_{SCR}$, a disulfide-bonded peptide that contains the amino acids of $fIX_{G4-Q11}$ but in a "scrambled" order (Table 1). Interestingly, $fIX_{SCR}$ competitively inhibited factor Xa formation with a 2-fold lower affinity than $fIX_{G4-Q11}$ (Figure 1B). One explanation for competition by the scrambled $\omega$-loop peptide $fIX_{SCR}$ is that positional alignment of specific residues within the constrained peptide is important for mediating a PS-dependent membrane interaction that competes with components of the factor Xase complex. A comparison of the $fIX_{G4-Q11}$ and $fIX_{SCR}$ sequences (Table 1) shows that the spatial proximity (four intervening residues) of two residues, Lys5 and Phe9, which we show below are involved in specific interactions between phosphatidylserine and $fIX_{G4-Q11}$, is maintained in the scrambled peptide (Phe4 and Lys8). These data suggest that the positioning of Phe relative to Lys in $fIX_{SCR}$ possibly preserves the presentation of important determinants necessary for mediating phosphatidylserine binding; however, the decreased affinity suggests other residues that are perturbed by the addition of C6PS are required, including Leu6, which has previously been shown to be involved in membrane binding (*18*). These data support other investigations which propose that both sequence position and spatial proximity play critical roles in defining the membrane binding properties of the vitamin K-dependent family of proteins (*37*). Of note, data of this type were not determined in the activated platelet system, which is complicated by many factors other than the phospholipid composition of the membrane surface (*20*).

*Three-Dimensional Structure of $fIX_{G4-Q11}$.* Circular dichroism (CD) was used to evaluate secondary structure changes of $fIX_{G4-Q11}$ that result from the presence of membrane-mimetic dodecylphosphocholine (DPC) micelles. The CD spectra of $fIX_{G4-Q11}$ in the presence and absence of DPC (Figure 2A) are similar, demonstrating that a PC-bearing membrane-mimetic environment does not significantly change the backbone conformation of this peptide. $^1$H NMR was used to further investigate the conformational response of $fIX_{G4-Q11}$ to DPC. The amide−α-proton (NH−αH) fingerprint region of TOCSY spectra of $fIX_{G4-Q11}$ in the presence of DPC exhibited modest backbone chemical shift perturbations for residues Glu8 and Lys5 (data not shown). Taken together, these data indicated that DPC micelles do not induce a conformational change in $fIX_{G4-Q11}$.

$^1$H TOCSY, DQF-COSY, and NOESY spectra of $fIX_{G4-Q11}$ in the presence of DPC at pH 5.6 and 15 °C were collected to determine the solution structure of $fIX_{G4-Q11}$ in this membrane-mimetic environment. Additional NOESY spectra collected at 25 °C ($H_2O$) and 15 °C (100% $D_2O$) permitted the assignment of proton resonances residing within or close to the bulk solvent peak. All of the proton resonances were assigned using canonical intraresidue spin system nomenclature with sequential connectivities completed through the use of αH and side chain proton connectivities to backbone amide (NH) protons of neighboring residues (*32*). The NH−αH proton or "fingerprint" region of a representative NOESY spectrum (Figure 2B) shows sequential residue αN($i$, $i$ + 1)

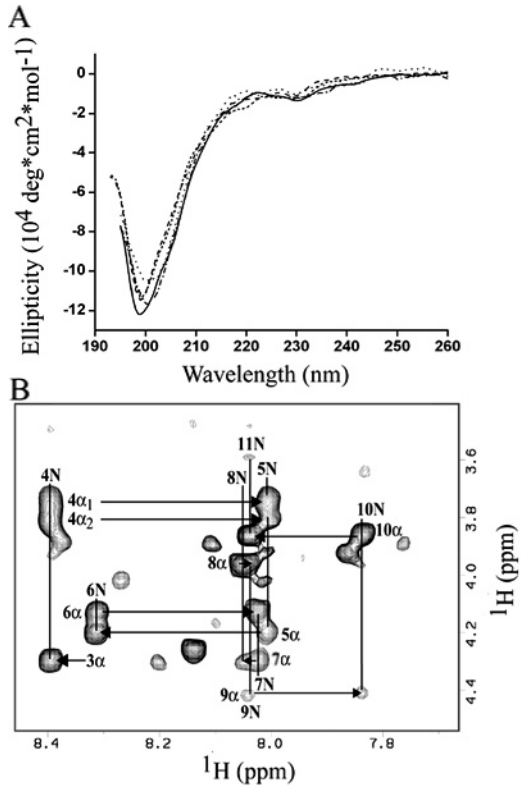


FIGURE 2: Circular dichroism and 2D $^1$H NMR spectral data of fIX$_{G4-Q11}$. (A) Circular dichroism spectra of the fIX$_{G4-Q11}$ peptide (67 $\mu$M) in phosphate buffer (pH 7.4) (—), DPC micelles (– – –), DPC micelles with 1.1 mM calcium (•••), $C_6$PS mixed DPC micelles (- - -), or phospholipid vesicles composed of 20% PS and 80% PC (-•-) at 37 °C are reported as molar ellipticity (degrees, square centimeter per mole). Spectra were recorded between 195 and 260 nm using a path length of 0.1 cm and a dwell time of 5 s/nm. Data are corrected by subtracting the respective buffer spectra with or without phospholipid. (B) The amide−α (NH−αH) fingerprint region of a 2D NOESY spectrum of fIX$_{G4-Q11}$ in the presence of 200 mM DPC-$d_{38}$ recorded at 15 °C with a mixing time of 350 ms is annotated to identify specific amino acids. The intraresidue NH−αH cross-peaks are labeled with the amino acid number (human FIX numbering). Arrowed-line connectivities are illustrated between intraresidue NH−αH and sequential αN($i$, $i$ + 1) cross-peaks throughout the peptide.

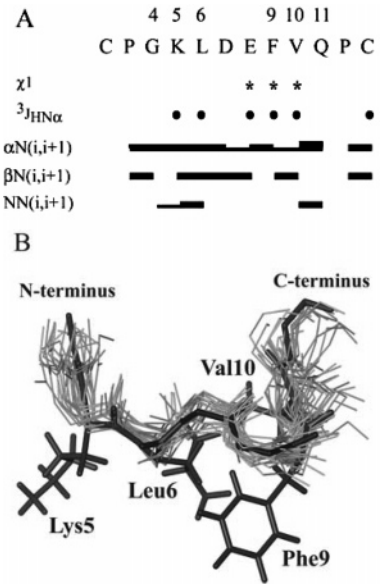


FIGURE 3: (A) Summary of sequential and short- to medium-range connectivities generated from NOE peaks. Bar thickness represents the intensity of the sequential and NN($i$, $i$ + 1), αN($i$, $i$ + 1), and $\beta$N($i$, $i$ + 1) NOE connectivities. Residues for which vicinal spin−spin coupling constants ($^3J_{NHα}$) were measured and used to calculate backbone $\phi$ torsion angles are marked with circles. Residues for which side chain $\chi_1$ angle restraints were determined are marked with an asterisk. (B) Overlay of 25 calculated structures of fIX$_{G4-Q11}$. All calculated backbone structures (gray) from residues Gly4−Gln11 (human FIX numbering) are shown superimposed using the backbone heavy atoms of the geometric average structure (black). The peptide backbone heavy atom rmsd compared to the geometric average structure is 0.84 Å for residues Gly4−Val10 and 1.08 Å for residues Gly4−Gln11. In addition to the N- and C-termini being labeled, the Lys5, Leu6, Phe9, and Val10 residues are labeled at the backbone peptide bond, and the side chain orientation of these residues in the average structure is shown.

connectivities observed throughout the peptide backbone. The proton resonance chemical shifts are presented in Table S-1 of the Supporting Information.

Following proton resonance assignments, short- and medium-range NOE interactions were defined from NOESY spectra. The observed NOE connectivities (summarized in Figure 3A) are congruent with the absence of α-helical or $\beta$-sheet structural elements in the CD data (Figure 2A). Backbone $\phi$ torsion angle conformations were calculated from $^3J_{HNα}$ coupling constants measured from amide proton cross-peak splittings in the resolution-enhanced DQF-COSY spectrum (*35*). Where possible, the $\chi_1$ rotamers were categorized by qualitative analysis of $\beta$-proton NOE intensities, $d_{αβ1}$, $d_{αβ2}$, $d_{Nβ1}$, and $d_{Nβ2}$ (*31*). Known distance restraints for the disulfide-bonded α-carbons, as well as paired distance restraints between the $\beta$-carbon of one cysteine and the sulfur atom of the other cysteine, were added according to Richardson et al. (*38*). Following a qualitative analysis of the penultimate family of calculated structures, the disulfide bond $\chi_3$ angle was restrained to the left-handed configuration (−90 ± 30°), which was predominant in this family of structures. Each proyl−peptide bond was configured trans based on the C$\beta$ and C$\gamma$ proline $^{13}$C chemical shift differences observed in a natural abundance $^{13}$C HSQC spectrum (*33*, *34*). All of these structural constraints were used as input for iterative simulated annealing and distance geometry calculations.

Twenty-five structures from the final family of fIX$_{G4-Q11}$ calculated structures were superimposed using the backbone heavy atoms of residues Gly4−Val10 (human factor IX numbering) (Figure 3B). The root-mean-square (rms) difference in the 25 structures calculated for the backbone heavy atoms of residues Lys5−Val10 was 0.92 Å. The average rmsd between these fIX$_{G4-Q11}$ structures and the calculated geometric average structure for the family is 1.08 Å for residues Gly4−Gln11. The side chains of Lys5, Leu6, and Phe9 are positioned along a common face of the $\omega$-loop-like structure; the Phe9 ring is oriented down, while the aliphatic side chain of Lys5 is positioned perpendicular to the plane of the loop (Figure 3B). The side chain of Val10 is on the backside of the cyclized loop roughly parallel in orientation to the side chain of Lys5. The backbone turn localized around Glu8 combined with the inward orientation of Asp7 exposes a distinct hydrophobic surface patch of the side chains from Lys5, Leu6, Phe9, and Val10.

*Calcium Ion-Independent Membrane-Binding Conformation of fIX$_{G4-Q11}$.* To access the calcium independence of the conformation provided by the proline-flanked, disulfide

bridge, CD was used to compare the secondary structure of $fIX_{G4-Q11}$ in DPC micelles with and without calcium. Near superimposition of the CD data (Figure 2A) demonstrates no change in the secondary structure of $fIX_{G4-Q11}$ following the addition of calcium. Similarly, TOCSY and NOESY data of $fIX_{G4-Q11}$ in DPC showed no backbone amide (NH), α-proton (Hα), or side chain proton chemical shift perturbations (data not shown) in the presence of calcium. Thus, $fIX_{G4-Q11}$ does not undergo a calcium-dependent conformational transition. CD was also used to compare the secondary structure of $fIX_{G4-Q11}$ in DPC micelles, in DPC micelles mixed with $C_6PS$, and in phospholipid vesicles. CD data (Figure 2A) show no secondary structure perturbation induced by DPC micelles, $C_6PS$/DPC micelles (13% $C_6PS$/87% DPC), or phospholipid vesicles (20% PS/80% PC), identifying that the secondary structure of the phospholipid-bound conformer of $fIX_{G4-Q11}$ is very similar to that of $fIX_{G4-Q11}$ in a DPC or $C_6PS$/DPC micelle environment.

*Interactions between $fIX_{G4-Q11}$ and Phosphatidylserine*. We added $C_6PS$ to DPC micelles to investigate interactions between $fIX_{G4-Q11}$ and phosphatidylserine. Interactions between $C_6PS$ and $fIX_{G4-Q11}$ were investigated using 2D $^1H$ NMR to monitor perturbations of $fIX_{G4-Q11}$ that are induced by $C_6PS$. TOCSY experiments were carried out with $fIX_{G4-Q11}$ solubilized in perdeuterated DPC (DPC-$d_{38}$) in the presence of increasing concentrations of protonated $C_6PS$. Superimposition of TOCSY fingerprint regions for three $C_6$-PS titration points (Figure 4A) reveals backbone NH−αH chemical shift perturbations for specific residues in $fIX_{G4-Q11}$ as a function of $C_6PS$ concentration. The absolute value of the chemical shift change observed for each peptide NH, Hα, and H$\beta$ resonance was measured (Figure 4B). When these chemical shift mapping data are represented as a stacked bar plot for each $fIX_{G4-Q11}$ residue, the most significant proton chemical shift perturbations are localized to Lys5, Leu6, Phe9, and Val10 of $fIX_{G4-Q11}$. These data demonstrate the localized sensitivity of these residues to increasing concentrations of $C_6PS$. These chemical shift data are represented by a single set of resonances for each amino acid, suggesting that the interaction of residues Lys5, Leu6, Phe9, and Val10 with $C_6PS$-containing micelles is in the fast exchange regime on the NMR time scale.

The interaction of $fIX_{G4-Q11}$ with $C_6PS$ was accompanied by a decreased rate of exchange of the NHζ side chain protons of Lys5 (data not shown). In the absence of $C_6PS$, the Lys5 side chain Hε−NHζ and Hγ−NHζ proton resonances are not observed in TOCSY data due to the mobility of this side chain and/or its rapid exchange with the bulk solvent. However, in the presence of increasing concentrations of $C_6PS$, the Hε−NHζ and Hγ−NHζ proton resonances are observed. These data combined with a concomitant chemical shift perturbation of both the Lys5 backbone and side chain support the possibility that Lys5 is involved in $C_6PS$ binding.

To further examine the interaction of $C_6PS$ with $fIX_{G4-Q11}$, 1D $^1H$ NMR spectra of $C_6PS$ were collected in the presence and absence of $fIX_{G4-Q11}$. Assignments of the $C_6PS$ resonances were made using $^1H$ spectra and TOCSY spectra collected for $C_6PS$/DPC micelles in the absence of peptide as well as previously reported NMR data of phosphatidylserine in DPC micelles (*39*, *40*). In the presence of $fIX_{G4-Q11}$, the Cβ$H$ $^1H$ resonance of the PS headgroup and

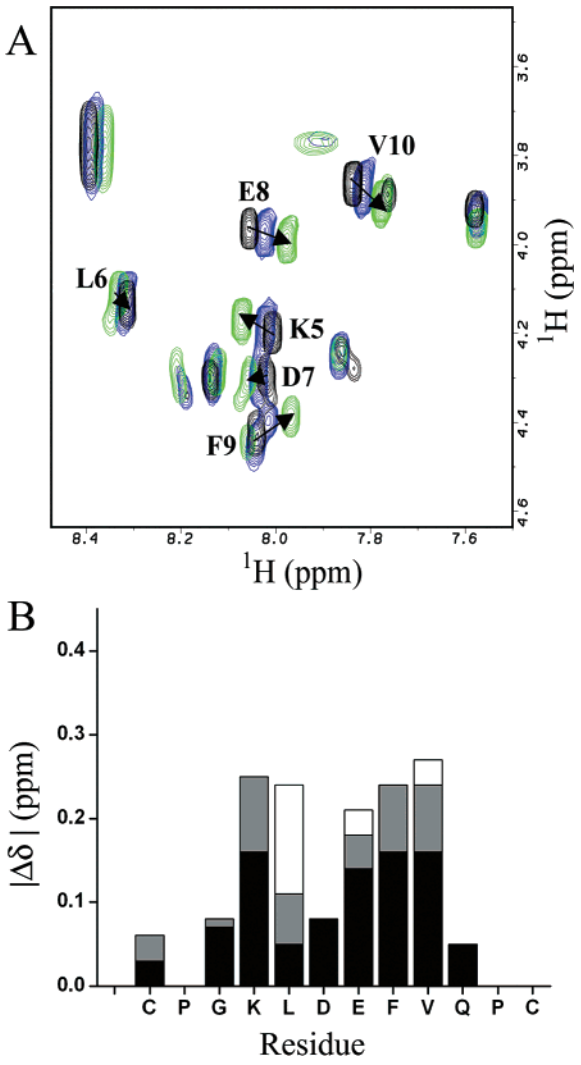


FIGURE 4: $C_6PS$ titration experiments monitored by chemical shifts of $fIX_{G4-Q11}$. (A) The NH−αH regions of three 2D TOCSY spectra of $fIX_{G4-Q11}$ in the presence of varying $C_6PS$ concentrations [0 (black), 8 (blue), and 14 mM (green)] in the presence of 200 mM DPC are superimposed. Each spectrum was collected in 90% $H_2O$ and 10% $D_2O$ at 15 °C with a mixing time of 45 ms. Those resonances that undergo chemical shift perturbations in the presence of $C_6PS$ are marked with the residue number (human FIX numbering) and an arrow indicating a downfield (←) or upfield (→) shift of the NH resonance. (B) The $fIX_{G4-Q11}$ residues that interact with $C_6PS$ are denoted with the absolute value of the change in NH [$|\delta_{NH(DPC)} - \delta_{NH(DPC+C6PS)}|$] (black), αH [$|\delta_{\alpha H(DPC)} - \delta_{\alpha H(DPC+C6PS)}|$] (gray), and βH [$|\delta_{\beta H(DPC)} - \delta_{\beta H(DPC+C6PS)}|$] (white) chemical shifts for all resonances of $fIX_{G4-Q11}$ in the presence of $C_6PS$ and DPC at a ratio of 1:5.

the $C1H_2$ and $C3H_2$ $^1H$ resonances of the glycerol backbone of $C_6PS$ were conformationally perturbed as noted by their enhanced spectral resolution (Figure 5). These findings indicate that the association of $fIX_{G4-Q11}$ with $C_6PS$ in DPC micelles changes the mobility, order, and/or structure of specific proton groups in the PS headgroup and glycerol backbone of $C_6PS$.

To further probe the interactions between $fIX_{G4-Q11}$ and $C_6PS$, we collected several 2D $^1H$ NOESY experiments aimed at detecting specific peptide−phospholipid NOEs. $fIX_{G4-Q11}$ was solubilized in $D_2O$ in the presence of perdeuterated DPC micelles and increasing concentrations of protonated $C_6PS$ (Figure 6). In the presence of $C_6PS$, several

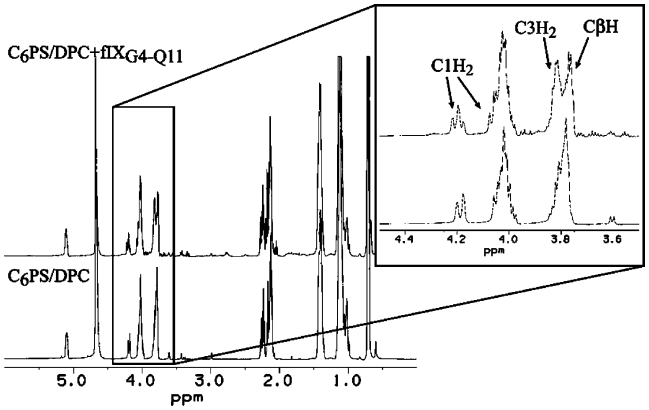


FIGURE 5: Perturbation of $C_6$PS protons by $fIX_{G4-Q11}$ as monitored by 1D $^1$H NMR. Select regions of the 1D $^1$H NMR spectra of protonated $C_6$PS in DPC-$d_{38}$ micelles (1:6.7 molar ratio) in the absence (bottom) and presence (top) of 3 mM $fIX_{G4-Q11}$ acquired at 15 °C. The region of the spectra between 3.5 and 4.4 ppm is expanded in the boxed inset. The C1H$_2$, C3H$_2$, and C$\beta$H peaks of $C_6$PS that are further resolved and perturbed in the presence of $fIX_{G4-Q11}$ are annotated.

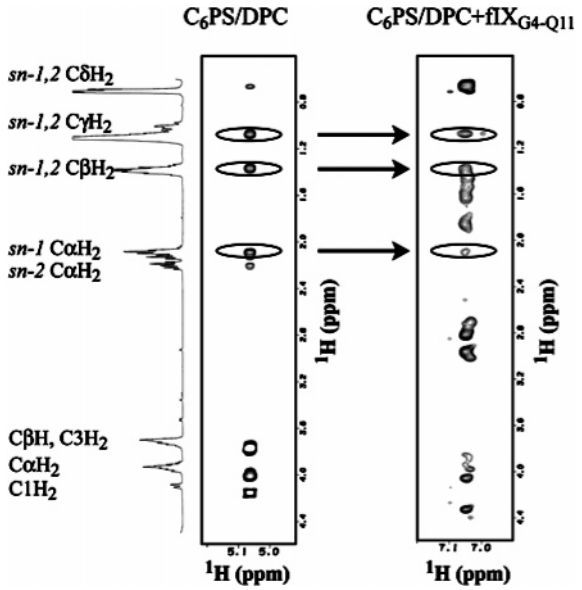


FIGURE 6: Interaction between Phe9 of $fIX_{G4-Q11}$ and $C_6$PS observed in 2D NOESY data. The 1D $^1$H NMR spectrum at the left (vertical) is that of protonated $C_6$PS in DPC-$d_{38}$ micelles (1:6.7 $C_6$PS:DPC molar ratio) in the absence of $fIX_{G4-Q11}$, and the proton resonances of $C_6$PS are labeled. In the first panel is a region (4.92−5.22 ppm) from the 2D NOESY spectrum of protonated $C_6$PS in deuterated DPC-$d_{38}$ micelles (at a 1:6.7 molar ratio) in the absence of $fIX_{G4-Q11}$; thus, only intra-phosphatidylserine resonances are observed, acquired at 15 °C with a mixing time of 350 ms. In the panel at the right is a region (6.9−7.2 ppm) from the 2D NOESY spectrum of protonated $C_6$PS in DPC-$d_{38}$ micelles in the presence of $fIX_{G4-Q11}$ acquired under these same conditions. NOE cross-peaks (circled) between specific $C_6$PS protons, namely, *sn*-1,2 C$\gamma$H$_2$, *sn*-1,2 C$\beta$H$_2$, and *sn*-1 C$\alpha$H$_2$, and the degenerate H$\delta$ and H$\epsilon$ aromatic ring protons (7.05 ppm) of the side chain of Phe9 in $fIX_{G4-Q11}$ are observed in this region of the NOESY spectrum. All other resonances in this panel are intrapeptide NOESY cross-peaks, either intraresidue cross-peaks of Phe9 or NOE cross-peaks between the Phe9 ring protons and other side chain or backbone $\alpha$H protons in $fIX_{G4-Q11}$.

new NOE cross-peaks were identified between the *sn*-1,2 C$\gamma$H$_2$ methylene groups, the *sn*-1,2 C$\beta$H$_2$ methylene groups, and the *sn*-1 C$\alpha$H$_2$ headgroup of $C_6$PS and the degenerate H$\delta$ and H$\epsilon$ protons of the aromatic side chain of Phe9. We were not able to discern potential NOE interactions between the *sn*-2 C$\alpha$H$_2$ or *sn*-1,2 C$\delta$H$_2$ methylene groups or the C$\beta$H $^1$H of $C_6$PS and the peptide due to the spectral degeneracy of these resonances with resonances endogenous to $fIX_{G4-Q11}$ itself. Nonetheless, the NOE data demonstrate that these $C_6$-PS acyl chain and/or headgroup protons reside within 3−6 Å of the Phe9 aromatic ring within this mixed micellar environment.

## DISCUSSION

We report the membrane binding properties and three-dimensional structure of $fIX_{G4-Q11}$, a membrane binding determinant of factor IXa. The membrane binding properties indicate that $fIX_{G4-Q11}$ contains an essential subset of the membrane-binding motif of intact factor IX. These structural studies reveal specific interactions between $fIX_{G4-Q11}$ and phosphatidylserine within a mixed-micelle system. The proline-flanked, disulfide bridge in $fIX_{G4-Q11}$ preserves the $\omega$-loop conformation in the absence of calcium. Notably, we observed $C_6$PS-dependent chemical shift perturbations in $fIX_{G4-Q11}$ that identify Lys5, Leu6, Phe9, and Val10 as residues that interact predominantly with phosphatidylserine. In addition, we determined that $C_6$PS in a DPC mixed micelle selectively protects the NH$\zeta$ side chain resonance of Lys5 from solvent exchange, indicating that this moiety interacts with or is sequestered from the bulk solvent only in the presence of $C_6$PS-containing micelles. NOEs between specific acyl chain and headgroup protons of $C_6$PS and the aromatic ring protons of Phe9 show that these phosphatidylserine protons reside 3−6 Å from Phe9. Additional evidence for this $C_6$PS-specific interaction is provided by data identifying the stabilization of the phosphoserine headgroup and glycerol backbone of $C_6$PS in the presence of $fIX_{G4-Q11}$. Taken together, these data provide sufficient spatial constraints to allow us to propose a model of the interaction of the factor IX peptide, $fIX_{G4-Q11}$, with phosphatidylserine.

Previous investigations by the laboratories of P. Walsh and others have identified residues within the factor IX Gla domain that facilitate both membrane and platelet binding (*18*, *41*, *42*). Residues within the $\omega$-loop, specifically residues 3−11, were shown to contribute to high-affinity binding of factor IX/factor IXa to activated platelets. Because of the lack of high-resolution structural information at that time, computer-generated models were used to rationally design a constrained synthetic peptide ($fIX_{G4-Q11}$) that included $\omega$-loop residues 4−11 (*20*).

Here we demonstrate that $fIX_{G4-Q11}$ inhibits binding of factor IXa to lipospheres (15% PS/20% PE/65% PC) with a $K_i$ of ∼11 $\mu$M. This factor IX $\omega$-loop-derived peptide competes with active site-labeled factor IXa for ∼60% of the phospholipid binding sites on these lipospheres, a percentage that is consistent with that reported for $fIX_{G4-Q11}$ competition on activated platelet binding sites (*20*). From their studies, Ahmed et al. concluded that the site to which $fIX_{G4-Q11}$ binds is the shared factor IX/factor IXa binding site on the surface of activated platelets. They reported that the $\omega$-loop peptide of factor IX, $fIX_{G4-Q11}$, mediates the binding of factor IX/factor IXa to sites on activated platelets (∼250−300 sites/platelet) that are independent of cofactor and substrate binding. The interactions that we observed

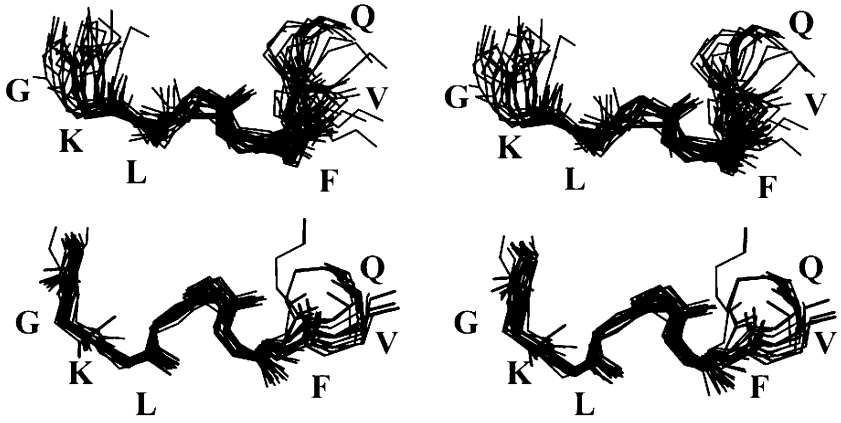


FIGURE 7: Comparison of the backbone conformations of $fIX_{G4-Q11}$ and the calcium-bound FIX Gla domain, FIX(1−47). Stereoview images of 25 of the backbone conformations of $fIX_{G4-Q11}$ in DPC (top), residues Gly4−Gln11, and 17 previously published structures of the calcium-bound FIX Gla domain, FIX(1−47) (bottom), residues Gly4−Gln11 (*9*). The $fIX_{G4-Q11}$ and calcium-bound FIX(1−47) structures share a highly similar backbone fold over the factor IX Gla domain $\omega$-loop residues, Gly4−Gln11. The rms deviations between the backbone heavy atoms of residues Gly4−Leu6 and Phe9−Gln11 in the average structures of $fIX_{G4-Q11}$ and FIX(1−47)−$Ca^{2+}$ are 0.75 and 0.97 Å, respectively. The factor IX $\omega$-loop region residues are identified.

between $fIX_{G4-Q11}$ and phosphatidylserine by NMR are consistent with the notion that the shared factor IX/factor IXa binding site in our system of purified components is analogous to the phosphatidylserine-dependent binding site proposed by Walsh and colleagues in activated platelets.

Differences in the binding data obtained in our studies and those previously reported may be attributed to the complexity of the activated platelet system. Although it has not been clearly defined, it is possible that the factor IX/factor IXa binding site in an activated platelet system is comprised of PS lipid, a factor IX receptor, or other membrane binding determinants. It is now well established that it is not simply the exposure of a critical threshold of anionic phospholipids on a membrane surface but also the two-dimensional packing of headgroups, vesicle curvature, and other lipid and/or nonlipid components that have been previously detected in platelet preparations with ligand blotting techniques, but have remained elusive. Although there are many mechanistic explanations for what occurs on a platelet surface, it remains likely that the factor IX/factor IXa binding site in an activated platelet system is comprised of PS lipid, a factor IX receptor, or other membrane binding determinants, including but not limited to "receptors" for the cofactor, FVIIIa, and substrate FX which facilitate the formation of a 1:1 VIIIa−X complex that is in excess (4-fold) (*43*). A recent review has further speculated that each of the components in the FX-activating complex binds to a unique receptor site on the activated platelet membrane and the presence of the other components required for the conversion of FX to FXa significantly enhances the affinity and specificity of the others (*44*, *45*). Our system comprised of coagulant membrane-binding proteins, $CaCl_2$, and a membrane surface is not capable of recapitulating the complexity of the activated platelet system, which expresses these unique binding determinants. Of note, $fIX_{G4-Q11}$ inhibited the activation of factor X by factor IXa in the presence of factor VIII and phospholipid vesicles (20% PS/80% PC). A Dixon plot of these data confirmed that $fIX_{G4-Q11}$ is a competitive inhibitor with a $K_i$ of 285 ± 62 $\mu$M. These data are very similar to those determined elsewhere ($K_i$ = 165 ± 35 $\mu$M) in which $fIX_{G4-Q11}$ was a competitive inhibitor of factor Xa formation in the presence of the Xase complex on a platelet surface (*20*). In summary, these data suggest that $fIX_{G4-Q11}$ inhibits the functional Xase complex by competing for similar membrane binding sites in both our purified system and activated platelets (*20*).

The backbone structure of $fIX_{G4-Q11}$ and the analogous region of the calcium-bound factor IX Gla domain, FIX(1−47) (*9*), share a similar backbone fold with a rmsd for the backbone heavy atoms of $\omega$-loop residues Gly4−Leu6 of 0.75 Å and for $\omega$-loop residues Phe9−Gln11 of 0.97 Å. A stereoview of overlays of the $fIX_{G4-Q11}$ and calcium-bound FIX(1−47) structures in Figure 7 shows the consistency in backbone fold between the families of structures. Recent X-ray data of calcium-bound human FIX(1−47) in complex with Fab fragments derived from a humanized, conformation-specific anti-factor IX antibody identified a unique role for Gla7 in the factor IX Gla domain (*46*). Gla7 is critical for orienting the $\omega$-loop polypeptide backbone and stabilizing the positions of the amide nitrogens within the backbone for hydrogen bonding. Conservation of the polypeptide backbone conformation in calcium-bound FIX(1−47) and $fIX_{G4-Q11}$ in the absence of calcium verifies that the structurally stabilizing interactions between Gla residues and calcium in FIX(1−47) are supplanted by the proline-flanked, disulfide bond constraint in $fIX_{G4-Q11}$, providing a functional calcium ion-independent $\omega$-loop-like peptide.

Prior reports suggest that Lys5, Leu6, and Phe9 of factor IX and homologous residues in other vitamin K-dependent membrane-binding proteins also interact with phospholipid membranes. Substitution of a photoactivatable phenylalanine analogue for Leu6 and Phe9 in the factor IX Gla domain FIX(1−47) enabled cross-linking to phospholipid membranes, while similar substitutions at positions 25 and 46 did not (*18*). Site-directed mutagenesis of Leu5 and Leu8 in protein C abrogates binding to phospholipid vesicles and thus anticoagulant function (*16*, *17*). Insertion of a Tyr residue at position 4 in the factor VII Gla domain resulted in a 2-fold increase in the level of membrane binding (*47*). One possible explanation for the enhanced membrane binding was a direct contact between this Tyr side chain and the hydrophobic acyl chain region of the phospholipid membrane. Fluorescence quenching experiments carried out with the prothrombin Gla domain substituted with a tryptophan residue for phenylalanine 4, PT(1−46)F4W, demonstrated phosphatidylserine-

specific membrane binding and penetration of this residue into the interfacial phospholipid membrane region (*19*).

The proton−proton interactions that we observed between the aromatic side chain of Phe9 and the acyl chain of $C_6PS$ place the Phe9 ring within 5 Å of the $C_6PS$ lipid. Specifically, intramolecular NOEs between the H$\delta$ and H$\epsilon$ protons of Phe9 and the *sn*-1,2 C$\gamma H_2$ methylene groups, the *sn*-1,2 C$\beta H_2$ methylene groups, and the *sn*-1 C$\alpha H_2$ group of $C_6PS$ suggest the phosphatidylserine-specific association of $fIX_{G4-Q11}$ involves both the headgroup and the acyl chain. We observed a similar mechanism of Gla domain contact between the prothrombin $\omega$-loop and the phospholipid acyl chain of lysoPS in our recently published crystal structure of bovine prothrombin [PT(1−46)−$Ca^{2+}$−lysoPS (*12*)]. In the prothrombin ternary complex, the *sn*-1 acyl chain of lysoPS is in van der Waals contact with the phenylalanine at position 5 in the prothrombin Gla domain. The importance of the Phe9 interaction in factor IX is illustrated by previous studies identifying that point mutations involving Phe9 (Phe9Ala and Phe9Met) result in a factor IX protein that does not bind to activated platelets (*42*). In addition, the importance of these critical Phe9 interactions is observed in a naturally occurring genetic mutation, Phe9Ile in patients with hemophilia B (*48*). These patients have normal factor IXa protein levels but low factor IX activity. We hypothesize that the abnormality is due to abnormal phosphatidylserine binding.

Our data indicate that the $C_6PS$ phosphoserine headgroup C$\beta$H proton and glycerol backbone C1$H_2$ and C3$H_2$ methylene protons are stabilized in the presence of $fIX_{G4-Q11}$. These data are best explained by the spatial proximity between $fIX_{G4-Q11}$ $\omega$-loop residues and the glycerophosphoserine motif of $C_6PS$, and are supported by our recent studies with the prothrombin Gla domain in complex with lysophosphatidylserine [PT(1−46)−$Ca^{2+}$−lysoPS (*12*)]. Following phospholipid binding, the prothrombin Gla domain $\omega$-loop is rigidly structured, the result of several interactions between both the glycerol backbone and acyl chain of lysoPS and residues within this region, including Lys3. Hydrogen bond and salt bridge interactions between the acyl and phosphoryl ester oxygens of the lipid glycerophosphate backbone and the NH$\zeta$ group of Lys3 conformationally fix this side chain.

Our data in this investigation show protection of the Lys5 NH$\zeta$ side chain protons from solvent exchange in the presence of $C_6PS$, indicating that Lys5 is involved in phosphatidylserine binding, a role that is consistent with the X-ray structure of calcium-bound human FIX(1−47) in complex with a humanized, conformation-specific anti-FIX antibody (*46*). In this complex, Lys5 within the factor IX Gla domain is a surface-exposed residue without a structural role in the factor IX Gla domain and the aliphatic side chain of Lys5 makes hydrophobic contacts with the CDR loops of the antibody. While these authors hypothesized that Lys5 in factor IX could bind phosphatidylserine in a manner analogous to that of Lys3 in the bovine prothrombin crystal structure [PT(1−46)−$Ca^{2+}$−lysoPS (*12*)], our data show the involvement of the $fIX_{G4-Q11}$ Lys5 NH$\zeta$ side chain protons in phosphatidylserine binding.

In addition to the potential hydrophobic contribution to membrane binding by the aliphatic side chain of Lys5, it is well established that the net charge and thus surface presentation of cationic residues such as lysine and arginine

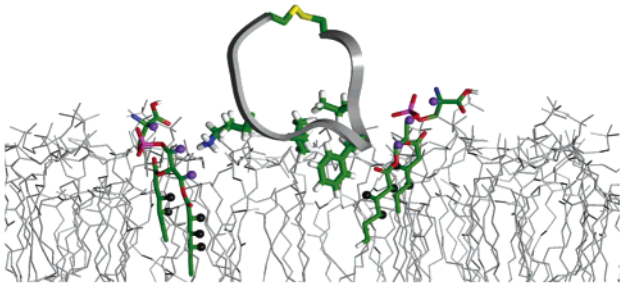

FIGURE 8: Model of $fIX_{G4-Q11}$ interacting with phosphatidylserine in a membrane-mimetic environment. Interaction between $fIX_{G4-Q11}$ and phosphatidylserine within a membrane surface is modeled on the basis of several structural features observed in our study, including proton chemical shift perturbation mapping of specific residues, protection of the Lys5 NH$\zeta$ side chain, NOE interactions between the aromatic ring of Phe9 and the acyl chain of dicaproylphosphatidylserine, and the stabilization of headgroup and glycerol backbone protons of $C_6PS$ by $fIX_{G4-Q11}$. The backbone of the $fIX_{G4-Q11}$ average structure is illustrated as a ribbon (gray); the Lys5, Leu6, Phe9, and Val10 side chains are rendered in stick representation and colored according to atom type, and monomers of $C_6PS$ that are interdigitated into a phosphatidylcholine membrane surface are rendered in stick representation colored according to atom type. Lipid protons participating in observed NOE contacts are highlighted in black, and $C_6PS$ proton groups stabilized by $fIX_{G4-Q11}$ are highlighted in purple. The membrane surface was modified from a phospholipid membrane surface and adapted to this investigation using molecular dynamics simulation (*54*).

that possess amino ($NH^{3+}$) and guanidinium ($CN^3H^5$) groups, respectively, are potential H-bond donors for anionic phospholipids within the membrane environment (*49*, *50*). In the pH range investigated in our study (5.6−7.5), the side chain of Lys5 is expected to be positively charged and thus may be involved in H-bonding or electrostatic salt bridge interactions, as recently determined for the high-affinity interaction of mitochondrial creatine kinase with the dianionic headgroup of cardiolipin (*51*). Furthermore, studies with another vitamin K-dependent protein, activated protein C, demonstrated a cardiolipin-dependent enhancement in the anticoagulant activity of the anticoagulant protein C complex which was attributed to an increased affinity for this anionic membrane environment (*52*). More importantly, a naturally occurring genetic mutation in patients with hemophilia B, Lys5Glu, which removes this critical NH$\zeta$ moiety, results in normal factor IXa protein levels, but low factor IX activity (*53*), possibly due to a loss or decrease of membrane binding potential and thus complex assembly. Taken together, these data identify an important role for the side chain of Lys5 in the factor IX Gla domain.

The observed interactions between the $\omega$-loop residues in $fIX_{G4-Q11}$ and $C_6PS$ were used to generate a representative model of $fIX_{G4-Q11}$ interacting with $C_6PS$ on a membrane surface (Figure 8). The peptide−$C_6PS$ contacts that were demonstrated in these studies and used to constrain the model are highlighted. Specifically, the backbone of $fIX_{G4-Q11}$ residues Lys5, Leu6, and Phe9 is positioned in a plane perpendicular to that of the oriented lipid and near the interfacial region of the membrane. Two molecules of $C_6PS$ are used to satisfy the observed peptide−$C_6PS$ contacts; however, a single $C_6PS$ molecule positioned between the side chains of Lys5 and Phe9 may also satisfy the constraints of the interaction. In addition, $C_6PS$ is positioned within the membrane in a manner that best fits the observed interaction

between specific phosphoserine headgroup and glycerol backbone protons of $C_6$PS and $fIX_{G4-Q11}$.

In summary, this work supports the idea that the factor IX $\omega$-loop is essential for phospholipid binding and identifies the phosphatidylserine-specific interactions of Lys5 and Phe9 in factor IX. Although the Gla domain sequences are highly conserved among the various vitamin K-dependent proteins, the dissociation constant for binding to model membranes varies by as much as 3 orders of magnitude (*6*). Lysine and phenylalanine at positions 5 and 9, respectively, are unique to the factor IX Gla domain sequence when compared with other vitamin K-dependent Gla domains, and thus, the specific phosphatidylserine interactions described here may be unique to factor IX. Further structural investigations may provide new insight into phospholipid structure-specific interactions with the Gla domains and the manner in which these impact the physiologic function.

## ACKNOWLEDGMENT

We thank M. Bern (Protein Core Facility, Tufts University School of Medicine, Boston, MA) and M. Jacobs (Division of Hemostasis and Thrombosis, Protein Core Facility, Beth Israel Deaconess Medical Center) for peptide synthesis.

## SUPPORTING INFORMATION AVAILABLE

$^1$H chemical shift assignments of $fIX_{G4-Q11}$. This material is available free of charge via the Internet at http://pubs.acs.org.

## REFERENCES

1. Gilbert, G. E., and Arena, A. A. (1996) Activation of the factor VIIIa-factor IXa enzyme complex of blood coagulation by membranes containing phosphatidyl-L-serine, *J. Biol. Chem. 271*, 11120−11125.
2. Furie, B., and Furie, B. C. (1988) The molecular basis of blood coagulation, *Cell 53*, 505−518.
3. Zwaal, R. F. A., Comfurius, P., and Bevers, E. M. (1998) Lipid−protein interactions in blood coagulation, *Biochim. Biophys. Acta 1376*, 433−453.
4. Dahlback, B. (2000) Blood coagulation, *Lancet 355*, 1627−1632.
5. Stenflo, J., and Dahlback, B. (2001) in *The molecular basis of blood disease* (Stamatoyannopoulus, G., Majerus, P. W., Perlmutter, R. M., and Varmus, H., Eds.) pp 579−613, W. B. Saunders, London.
6. McDonald, J. F., Shah, A. M., Schwalbe, R. A., Kisiel, W., Dahlback, B., and Nelsestuen, G. L. (1997) Comparison of naturally occurring vitamin K-dependent proteins: correlation of amino acid sequences and membrane binding properties suggests a membrane contact site, *Biochemistry 36*, 5120−5127.
7. Kalafatis, M., Egan, J. O., van't Veer, C., Cawthern, K. M., and Mann, K. G. (1997) The regulation of clotting factors, *Crit. Rev. Eukaryotic Gene Expression 7*, 241−280.
8. Furie, B., Bouchard, B. A., and Furie, B. C. (1999) Vitamin K-dependent biosynthesis of $\gamma$-carboxyglutamic acid, *Blood 93*, 1798−1808.
9. Freedman, S. J., Furie, B. C., Furie, B., and Baleja, J. D. (1995) Structure of the calcium ion-bound $\gamma$-carboxyglutamic acid-rich domain of factor IX, *Biochemistry 34*, 12126−12137.
10. Banner, D. W., D'Arcy, A., Chene, C., Winkler, F. K., Guha, A., Konigsberg, W. H., Nemerson, Y., and Kirchhofer, D. (1996) The crystal structure of the complex of blood coagulation factor VIIa with soluble tissue factor, *Nature 380*, 41−46.
11. Mizuno, H., Fujimoto, Z., Atoda, H., and Morita, T. (2001) Crystal structure of an anticoagulant protein in complex with the Gla domain of factor X, *Proc. Natl. Acad. Sci. U.S.A. 98*, 7230−7234.
12. Huang, M., Rigby, A. C., Morelli, X., Grant, M. A., Huang, G., Furie, B., Seaton, B., and Furie, B. C. (2003) Structural basis of membrane binding by Gla domains of vitamin K-dependent proteins, *Nat. Struct. Biol. 10*, 751−756.
13. Lesczczysnki, J. F., and Rose, G. D. (1986) *Science 234*, 849−855.
14. Soriano-Garcia, M., Padmanabhan, K., de Vos, A. M., and Tulinsky, A. (1992) The $Ca^{2+}$ ion and membrane binding structure of the Gla domain of Ca-prothrombin fragment 1, *Biochemistry 31*, 680−685.
15. Fetrow, J. S. (1995) Omega loops: nonregular secondary structures significant in protein function and stability, *FASEB J. 9*, 708−717.
16. Zhang, L. C. F. J. (1994) The binding energy of human coagulation protein C to acidic phospholipid vesicles contains a major contribution from leucine 5 in the $\gamma$-carboxyglutamic acid domain, *J. Biol. Chem. 269*, 3590−3595.
17. Christiansen, W. T., Jalbert, L. R., Robertson, R. M., Jhingan, A., Prorok, M., and Castellino, F. J. (1995) Hydrophobic amino acid residues of human anticoagulation protein C that contribute to its functional binding to phospholipid vesicles, *Biochemistry 34*, 10376−10382.
18. Freedman, S. J., Blostein, M. D., Baleja, J. D., Jacobs, M., Furie, B. C., and Furie, B. (1996) Identification of the phospholipid binding site in the vitamin K-dependent blood coagulation protein factor IX, *J. Biol. Chem. 271*, 16227−16236.
19. Falls, L. A., Furie, B. C., Jacobs, M., Furie, B., and Rigby, A. C. (2001) The $\omega$-loop region of the human prothrombin $\gamma$-carboxyglutamic acid domain penetrates anionic phospholipid membranes, *J. Biol. Chem. 276*, 23895−23902.
20. Ahmad, S. S., Wong, M. Y., Rawala, R., Jameson, B. A., and Walsh, P. N. (1998) Coagulation Factor IX Residues G4−Q11 Mediate Its Interaction with a Shared Factor IX/IXa Binding Site on Activated Platelets but Not the Assembly of the Functional Factor X Activating Complex, *Biochemistry 37*, 1671−1679.
21. Habeeb, A. F. S. A. (1979) Reaction of protein sulfhydryl groups with Ellman's reagent, *Methods Enzymol.*, 457−464.
22. Johnson, S. M., Bangham, A. D., Hill, M. W., and Korn, E. D. (1971) Single layer liposomes, *Biochim. Biophys. Acta 233*, 820−826.
23. Lollar, P., and Fass, D. N. (1984) Inhibition of activated porcine factor IX by dansyl-glutamyl-glycyl-arginyl-chloromethyl ketone, *Arch. Biochem. Biophys. 233*, 438−446.
24. Gilbert, G. E., Drinkwater, D., Barter, S., and Clouse, S. B. (1992) Specificity of phosphatidylserine-containing membrane binding sites for factor VIII: studies with model membranes supported by glass microspheres (lipospheres), *J. Biol. Chem. 267*, 15861−15868.
25. Cheng, Y., and Prusoff, W. H. (1973) Relationship between the inhibition constant ($K_I$) and the concentration of inhibitor which causes 50% inhibition ($I_{50}$) of an enzymatic reaction, *Biochem. Pharmacol. 22*, 3099−3108.
26. Burri, B., Edgington, T., and Fair, D. (1987) Molecular interactions of the intrinsic activation complex of coagulation: binding on native and activated human factors IX and X to defined phospholipid vesicles, *Biochim. Biophys. Acta 923*, 176−186.
27. Ahmad, S. S., Rawala-Sheikh, R., and Walsh, P. N. (1989) Platelet receptor occupancy with factor IXa promotes factor X activation, *J. Biol. Chem. 264*, 20012−20016.
28. Levitt, M., Freeman, R., and Frenkiel, T. (1982) Broadband heteronuclear decoupling, *J. Magn. Reson. 47*, 328.
29. Bax, A., and Davis, D. G. (1985) MLEV-17 based two-dimensional homonuclear magnetization transfer spectroscopy, *J. Magn. Reson. 65*, 355−360.
30. Clore, G. M., and Gronenborn, A. M. (1989) Determination of three-dimensional structures of proteins and nucleic acids in solution by nuclear magnetic resonance spectroscopy, *Crit. Rev. Biochem. Mol. Biol. 24*, 479−564.
31. Roberts, G. C. K. e. (1993) *NMR of macromolecules: A practical approach*, Oxford University Press, Oxford, U.K.
32. Wuthrich, K. (1986) *NMR of Proteins and Nucleic Acids*, John Wiley & Sons, New York.
33. Richarz, R., and Wurthrich, K. (1978) Carbon-13 NMR chemical shifts of the common amino acid residues measured in aqueous solutions of the linear tetrapeptides H-Gly-Gly-X-L-Ala-OH, *Biopolymers 17*, 2133−2141.
34. Schwarzinger, S., Kroon, G. J. A., Foss, T. R., Wright, P. E., and Dyson, H. J. (2000) Random coil chemical shifts in acidic 8 M urea: implementation of random coil shift data in NMRview, *J. Biomol. NMR 18*, 43−48.
35. Havel, T. F. (1991) in *Progress in Biophysics and Molecular Biology* (Nobel, D., and Blundell, T. F., Eds.) pp 43−78, Pergamon Press, Oxford, U.K.

36. Jacobs, M., Freedman, S. J., Furie, B. C., and Furie, B. (1994) Membrane binding properties of the factor IX $\gamma$-carboxyglutamic acid-rich domain prepared by chemical synthesis, *J. Biol. Chem. 268*, 25494−25501.
37. Sun, Y. H., Shen, L., and Dahlback, B. (2003) Gla domain-mutated human protein C exhibiting enhanced anticoagulant activity and increased phospholipid binding, *Blood 101*, 2277−2284.
38. Richardson, J. S. (1981) The Anatomy and Taxonomy of Protein Structure, *Adv. Protein Chem. 34*, 167−339.
39. Sanson, A., Monck, M. A., and Neumann, J.-M. (1995) 2D $^1$H NMR conformational study of phosphatidylserine diluted in perdeuterated dodecylphosphocholine micelles. Evidence for a pH-induced conformational transition, *Biochemistry 24*, 5938−5944.
40. Mousson, F., Coic, Y.-M., Baleux, F., Beswick, V., Sanson, A., and Neumann, J.-M. (2002) Deciphering the role of individual acyl chains in the interaction network between phosphatidylserines and a single-spanning membrane protein, *Biochemistry 41*, 13611−13616.
41. Ahmad, S. S., Rawala-Sheikh, R., Cheung, W. F., Jameson, B. A., Staford, D. W., and Walsh, P. N. (1994) High-affinity, specific factor IXa binding to platelets is mediated in part by residues 3−11, *Biochemistry 33*, 12048−12055.
42. Melton, L. G., Li, T., Stafford, D. W., and Gabriel, D. A. (2001) Location of the platelet binding site in zymogen coagulation factor IX, *Blood Coagulation Fibrinolysis 12*, 237−243.
43. Ahmad, S. S., and Walsh, P. N. (2002) Coordinate binding studies of the substrate (factor X) with the cofactor (factor VIII) in the assembly of the factor X activating complex on the activated platelet surface, *Biochemistry 41*, 11269−11276.
44. Ahmad, S. S., London, F. S., and Walsh, P. N. (2003) Binding studies of the enzyme (factor IXa) with the cofactor (factor VIIIa) in the assembly of factor-X activating complex on the activated platelet surface, *J. Thromb. Haemostasis 1*, 2348−2355.
45. Ahmad, S. S., London, F. S., and Walsh, P. N. (2003) The assembly of the factor X-activating complex on activated human platelets, *J. Thromb. Haemostasis 1*, 48−59.
46. Huang, M., Furie, B. C., and Furie, B. (2004) Crystal Structure of the calcium-stabilized human factor IX gla domain bound to a conformation-specific anti-factor IX antibody, *J. Biol. Chem. 279*, 14338−14346.
47. Harvey, S. B., Stone, M. D., Martinez, M. B., and Nelsestuen, G. L. (2003) Mutagenesis of the $\gamma$-carboxyglutamic acid domain of human factor VII to generate maximum enhancement of the membrane contact site, *J. Biol. Chem. 278*, 8363−8369.
48. Saad, S., Rowley, G., Tagliavacca, L., Green, P. M., and Giannelli, F. (1994) First report on UK database of *Haemophilia* B mutations and pedigrees. UK *Haemophilia* Centres, *Thromb. Haemostasis 71*, 563−570.
49. Gelb, M. H., Cho, W., and Wilton, D. C. (1999) Interfacial binding of secreted phospholipases A2: more than electrostatics and a major role for tryptophan, *Curr. Opin. Struct. Biol. 9*, 428−432.
50. Nelsestuen, G. L., and Ostrowski, B. G. (1999) Membrane association with multiple calcium ions: vitamin-K-dependent proteins, annexins, and pentraxins, *Curr. Opin. Struct. Biol. 9*, 433−437.
51. Schlattner, U., Gehring, F., Vernoux, N., Tokarska-Schlattner, M., Neumann, D., Marcillat, O., Vial, C., and Wallimann, T. (2004) C-terminal lysines determine phospholipid interaction of sarcomeric mitochondrial creatine kinase, *J. Biol. Chem. 279*, 24334−24342.
52. Fernandez, J. A., Kojima, K., Petaja, J., Hackeng, T. M., and Griffin, J. H. (2000) Cardiolipin enhances protein C pathway anticoagulant activity, *Blood Cells Mol. Dis. 26*, 115−123.
53. Rowley, G., Saad, S., Giannelli, F., and Green, P. M. (1995) Ultrarapid mutation detection by multiplex, solid-phase chemical cleavage, *Genomics 30*, 574−582.
54. Heller, H., Schaefer, M., and Schulten, K. (1993) Molecular dynamics simulation of a bilayer of 200 lipids in the gel and in the liquid crystal phase, *J. Phys. Chem. 97*, 8343−8360.

BI049107F